Available online at www.sciencedirect.com
SCIENCE DIRECT®
ELSEVIER
Solar Energy 75 (2003) 285–293
SOLAR ENERGY
www.elsevier.com/locate/solener

Combined non-gray radiative and conductive heat transfer in solar collector glass cover

Maatouk Khoukhi [a,*], Shigenao Maruyama [a], Seigo Sakai [a], Masud Behnia [b]

[a] *Institute of Fluid Science, Tohoku University, Katahira 2-1-1, Aoba-ku, Sendai 980-8577, Japan*
[b] *University of Sydney, NSW 2006, Australia*

Received 4 November 2002; accepted 11 August 2003

Abstract

A rigorous approach for the radiative heat transfer analysis in solar collector glazing is developed. The model allows a more accurate prediction of thermal performance of a solar collector system. The glass material is analysed as a non-gray plane-parallel medium subjected to solar and thermal irradiations in the one-dimensional case using the Radiation Element Method by Ray Emission Model (REM by REM).

This method is used to analyse the combined non-gray convective, conductive and radiative heat transfer in glass medium. The boundary surfaces of the glass are specular. The spectral dependence of the relevant radiation properties of glass (i.e. specular reflectivity, refraction angle and absorption coefficient) are taken into consideration. Both collimated and diffuse incident irradiation are applied at the boundary surfaces using the spectral solar model proposed by Bird and Riordan. The optical constants of a commercial ordinary clear glass material have been used. These optical constants (100 values) of real and imaginary parts of the complex refractive index of the glass material cover the range of interest for calculating the solar and thermal radiative heat transfer through the solar collector glass cover. The model allows the calculation of the steady-state heat flux and temperature distribution within the glass layer. The effect of both conduction and radiation in the heat transfer process is examined. It has been shown that the real and imaginary parts of the complex refractive index have a substantial effect on the layer temperature distribution. The computational time for predicting the combined heat transfer in such a system is very long for the non-gray case with 100 values of n and k. Therefore, a simplified non-gray model with 10 values of n and k and two semi-gray models have been proposed for rapid computations. A comparison of the proposed models with the reference non-gray case is presented. The result shows that 10 bandwidths could be used for rapid computation with a very high level of accuracy.
© 2003 Elsevier Ltd. All rights reserved.

1. Introduction

The radiative analysis of solar collectors is still difficult, even though the theoretical simplified approach has been available for many decades (Duffie and Beckman, 1974). Accurate prediction of thermal radiation in solar collector glass cover is of a great importance to achieve rigorous models that can be used to simulate the real behaviour of a solar collector. Indeed, the accurate prediction of the thermal performance of a solar collector system depends strongly on how the transparent glass-cover material is analysed.

Almost all the classical studies assume that the solar collector glass cover is transparent for the visible spectrum and nearly opaque to radiation at infrared wavelengths. Under such assumptions the optical analysis of the transparent cover can be found in many references (e.g. Howell et al., 1982; Duffie and Beckman, 1974). These assumptions may lead to considerable error in evaluating the thermal properties, heat flux and temperature distribution within the glass cover. In reality,

* Corresponding author. Tel./fax: +81-022-217-5244.
E-mail address: kmaatouk@pixy.ifs.tohoku.ac.jp (M. Khoukhi).

0038-092X/$ - see front matter © 2003 Elsevier Ltd. All rights reserved.
doi:10.1016/j.solener.2003.08.027

Nomenclature

A_i^{R}	effective radiation area [m^2]
c	specific heat [J kg^{-1} K^{-1}]
e_{air}	thickness of the air layer between the glass and the absorber [m]
$F_{i,j}^{\mathrm{A}}$	absorption view factor from element i to j
$G_{i,\lambda}$	incident radiation [W m^{-2}]
Gr	Grashoff number
h_{in}	inside convective heat transfer coefficient [W m^{-2} K^{-1}]
h_{out}	outside convective heat transfer coefficient [W m^{-2} K^{-1}]
I_λ	radiation intensity [W m^{-2} μm sr]
$I_{\mathrm{b},\lambda}$	blackbody radiation intensity [W m^{-2} μm sr]
k	imaginary part of the complex refractive index of element i of glass [–]
n	real part of the complex refractive index of element i of glass [–]
N	number of volume and surface elements
Nu	Nusselt number
Pr	Prandtl number
Q_J	diffuse radiosity heat transfer rate [W]
Q_T	heat transfer rate of emissive power [W]
Q_X	net rate of heat generation [W]
q_{r}	radiative heat flux [W m^{-2}]
q_X	net rate of heat generation per unit volume or unit surface [W m^{-3}, W m^{-2}]
$\vec{r}$	position vector, Fig. 1
R	ratio of CPU time consumed by the considered model to the CPU time consumed by the reference one
$\hat{s}$	unit direction vector, Fig. 1
S	path length through element.
S_{h}	heat generation source [W m^{-3}]
t	time [s]
T	temperature [K]
T_{abs}	absorber temperature [K]
$T_o(nl)$	absorber side glass temperature [K]
v	wind speed [ms^{-1}]
V_i	volume of the radiation element

Greek symbols

β	slope [°]
Δx_i	element thickness [m]
ε_i	emissivity
κ_λ	absorption coefficient of the glass [m^{-1}]
Λ	thermal conductivity [W m^{-1} K^{-1}]
μ	direction cosine of polar angle
μ_k	discretized angle
ν	kinematic viscosity [m^2 s^{-1}]
ρ	density of the glass material [kg m^{-3}]
σ	Stefan–Boltzman constant [W m^{-2} K^{-4}]
$\sigma_{\mathrm{s},\lambda}$	scattering coefficient
θ	polar angle, Fig. 3
θ_0	incident angle of collimated solar irradiation, Fig. 3
ζ	zenith angle [°]
w	solid angle
w_k	weight of discretized angle
Ω_i^{D}	Albedo of volume element or diffusivity of surface element

Subscripts

abs	absorber
b	blackbody
g	glass
i	element i
j	element j
λ	spectral value

the transmittance, like reflectance and absorbance, is a function of wavelength, angle of incidence of the incoming radiation, the real part n and the imaginary part k of the complex refractive index of the glass cover. Moreover, the real and imaginary parts of the complex refractive index of glass are spectrally dependent. But for most solar energy applications they are assumed to be wavelength independent.

In the present work, the cover of the solar collector is considered to be a participating non-gray media subjected to solar irradiation (specified by the spectral solar model proposed by Bird and Riordan (1986)) and thermal radiation (specified by blackbody emission of the outside environment and infrared radiation of the black absorber). A more refined and rigorous approach is applied using the Radiation Element Method by Ray Emission Model (REM by REM). The REM by REM is a generalized method for calculating radiation heat transfer between absorbing, emitting and scattering media. The boundary surfaces of the glass are specular and the spectral dependence of radiation properties such as specular reflectivity, refraction angle and absorption coefficient are all taken into consideration. The REM by REM method was proposed by Maruyama and Aihara (1997) and can be applied for complicated three-dimensional shapes. Further, Maruyama (1997, 1998) also applied this method for radiative heat transfer in anisotropic scattering parallel plane and a fog medium.

Heat transfer by combined conduction and radiation in glass medium has been studied by numerous researchers. For instance, Kong and Viskanta (1999) have compared the diffusion approximation and discrete ordinate method (DOM) for determining heat transfer in glass. The effect of the refractive index on radiative behaviour of heated absorbing–emitting layer has been reported by Spuckler and Siegel (1992). The combined conduction and radiation in two-layer planar medium with flux boundary conditions has been studied by Ho and Ozisik (1987).

In the work presented here an ordinary clear glass is considered and the optical constants of such material have been previously determined by Khoukhi et al. (2002, 2003) which comprises of 100 spectral values of n and k covering the range of solar and thermal radiation (0.3–24.5 μm). Using this data, the calculation has been performed for one position of the sun chosen at 11 a.m. on the fifth of July in Sendai city (Japan). The heat flux and temperature distribution within the glass layer have been obtained. For the case of non-gray assumption with 100 values of n and k the result is accurate but at the expense of a very long CPU time of about 28 h on a personal computer (VT-Alpha 600, 21164 A, 600 MHz). Hence, three non-gray models have been proposed and compared with the 100 bandwidths reference case (denoted here as NG100b). The first two models are semi-gray; one assumes the glass is transparent in the visible and near infrared and almost completely opaque to radiation in the infrared region (denoted here as SG1). The second model considers the glass is almost completely transparent in the visible and near infrared and partially opaque in the infrared region (denoted here as SG2). The third one is non-gray with 10 bandwidths (NG10b).

2. Method of analysis

The glass material is almost transparent to the solar radiation, due to the small value of k. On the other hand, the glass material is strongly absorbing in the infrared region. Therefore, the emission and absorption within a glass layer are taken into account.

2.1. Radiation transfer

The general form of the radiation intensity in direction $\hat{s}$ for a participating media is expressed from radiation energy balance as follows (Maruyama and Aihara, 1997):

$$\frac{\mathrm{d}I_\lambda(\vec{r},\hat{s})}{\mathrm{d}S} = -(\kappa_\lambda + \sigma_{\mathrm{s},\lambda})I_\lambda(\vec{r},\hat{s}) + \kappa_\lambda I_{\mathrm{b},\lambda}(T) + \frac{\sigma_{\mathrm{s},\lambda}}{4\pi} \times \int_{4\pi} I_\lambda(\vec{r},\hat{s}')P_\lambda(\hat{s}' \to \hat{s})\,\mathrm{d}w \tag{1}$$

where I_λ, κ_λ, $\sigma_{\mathrm{s},\lambda}$, d$w$, $I_{\mathrm{b},\lambda}$ and T are the radiation intensity, the spectral absorption, scattering coefficient, solid angle, blackbody radiation intensity and the temperature, respectively. $P_\lambda(\hat{s}' \to \hat{s})$ is a phase function from the direction $\hat{s}'$ to $\hat{s}$ (Maruyama and Aihara, 1997), S is the path length in the direction $\hat{s}$ and $\vec{r}$ is the position vector (see Fig. 1). A ray passing through the radiation element attenuates and separates into absorbed and transmitted fractions. The glass medium is discretized in thin element layer and considering the ith participating radiation element we introduce the following assumptions:

1. Each element is at a constant temperature.
2. The refractive index and heat generation rate per unit volume are also constants over each radiation element.
3. Scattering within the glass media is neglected.

Under such considerations and using the direction cosine of each ray, Eq. (1) becomes

$$\mu\frac{\mathrm{d}I_\lambda(x,\mu)}{\mathrm{d}x} = \kappa_\lambda[-I_\lambda(x,\mu) + I_{\mathrm{b},\lambda}(T)] \tag{2}$$

where μ is the direction cosine and x is the position through the thickness of the glass cover, $\mu \equiv cos\theta$ and θ is the polar angle (see Fig. 2).

The solution of the above equation is

$$I_\lambda(x+\Delta x_i,\mu) = I_{\mathrm{b},\lambda}(T)\left[1-\exp\left(\frac{-\kappa_\lambda\Delta x_i}{\mu}\right)\right] \tag{3}$$

Δx_i is the thickness of radiation element.

The radiant energy emitted from the element i can be approximated as

$$\mathrm{d}Q_{J,i,\lambda} = I_{\mathrm{b},\lambda}\cdot\mu\left[1-\exp\left(\frac{-\kappa_\lambda\Delta x_i}{\mu}\right)\right]\mathrm{d}w \tag{4}$$

Integrating over all solid angles, the spectral radiation energy from the radiation element i is given by

$$Q_{J,i,\lambda} = I_{\mathrm{b},\lambda}\sum_{k=1}^{K}\mu_k\left[1-\exp\left(\frac{-\kappa_\lambda\Delta x_i}{\mu_k}\right)\right]w_k \tag{5}$$

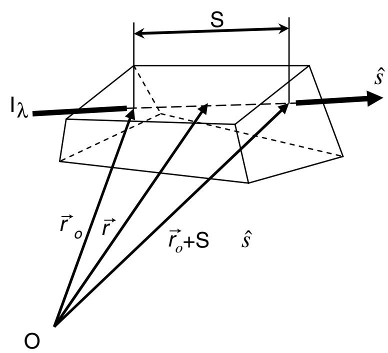

Fig. 1. Attenuation of radiation ray along the direction $\hat{s}$.

where μ_k, w_k and K are the discretized angle, the weight and the total number of discretized directions, respectively.

The effective area is given by the following expression (Maruyama and Aihara, 1997):

$$A_i^{\mathrm{R}} = \frac{1}{\pi}\sum_{k=1}^{K}\mu_k\left[1-\exp\left(\frac{-\kappa_\lambda \Delta x_i}{\mu_k}\right)\right]w_k \tag{6}$$

The diffuse radiosity heat transfer rate $Q_{J,i,\lambda}$ is expressed as

$$Q_{J,i,\lambda} = A_i^{\mathrm{R}}\varepsilon_i n^2\sigma T^4 + A_i^{\mathrm{R}}\Omega_i^{\mathrm{D}}G_{i,\lambda} \tag{7}$$

where ε_i, n and σ are the emissivity of the glass, real part of the complex refractive index of the glass and Stefan Boltzman constant. Ω_i^{D} is the albedo of volume element or diffusivity of surface element, reflectivity as defined by Maruyama and Aihara (1997) and $G_{i,\lambda}$ is the spectral irradiance on radiation element i.

The net rate of heat generation can be derived from the heat balance on the radiation element as (Maruyama and Aihara, 1997):

$$Q_{X,i,\lambda} = A_i^{\mathrm{R}}\varepsilon_i(n^2\sigma T^4 - G_{i,\lambda}) \tag{8}$$

If the system is consisted of N volume and surface elements ($N-2$ participating layers and two boundary surfaces), the Eqs. (7) and (8) can be rewritten as (Maruyama and Aihara, 1997):

$$\begin{aligned} Q_{J,i,\lambda} &= Q_{T,i,\lambda} \\ Q_{X,i,\lambda} &= Q_{T,i,\lambda} - \sum_{j=1}^{N}F_{j,i}^{\mathrm{A}}Q_{J,j,\lambda} \end{aligned} \tag{9}$$

In which, the absorption view factor $F_{j,i}^{\mathrm{A}}$ is introduced as defined by Maruyama and Aihara (1997), and the diffuse radiosity heat transfer rate $Q_{J,i,\lambda}$ is equal to the emissive power $Q_{T,i,\lambda}$, because the scattering Ω_i^{D} is neglected.

The heat transfer rate of spectral emissive power $Q_{T,i,\lambda}$ or the net rate of heat generation $Q_{X,i,\lambda}$ for each radiation element is given arbitrary as a boundary conditions (Maruyama and Aihara, 1997). The unknown $Q_{T,i,\lambda}$ or $Q_{X,i,\lambda}$ can be obtained by solving Eq. (9).

The total net rate of heat generation is given by

$$Q_{X,i} = \int_0^\infty Q_{X,i,\lambda}\,\mathrm{d}\lambda \tag{10}$$

The heat generation rate per unit volume is

$$q_{X,i} = Q_{X,i}/V_i \tag{11}$$

V_i is the volume of the radiation element.

The radiation heat flux through the layer is derived as (Maruyama (1998)):

$$q_{\mathrm{r},\lambda}(x) = q_{X,1} + \sum_{i=2}^{n}(q_{X,\lambda,i}\,\Delta x_i) \tag{12}$$

$q_{x,1}$ includes the blackbody emission emanating from the ambient, and the diffuse and direct solar radiation components.

2.2. Model analysis

Figs. 2 and 3 show the models of solar collector glass cover and solar collector system, respectively. The solar collector glazing is subjected to collimated and diffuse solar and thermal irradiations. The outside and absorber temperatures are 300 and 343 K, respectively. The convection is taken into consideration as boundary conditions in both sides of the glass and the thermal conductivity of the glass material is assumed to be constant. The outside convective heat transfer coefficient h_{out} is calculated using the empirical equation proposed by Watmuff (Agarwal and Larson, 1981):

$$h_{\mathrm{out}} = 2.8 + 3v \tag{13}$$

where v is the wind speed.

The convective heat transfer coefficient between the glass and the absorber h_{in} is determined by the following equations, assuming the natural convection of the air between two parallel planes (Duffie and Beckman, 1974).

$$h_{\mathrm{in}} = \frac{Nu\Lambda_{\mathrm{air}}}{e_{\mathrm{air}}} \tag{14}$$

Λ_{air} and e_{air} are the thermal conductivity and the thickness of the air layer between the glass and the absorber, respectively.

The *Nusselt* number is given by the following relation (Duffie and Beckman, 1974):

$$Nu = [0.06 - 0.017(\beta/90)]Gr^{1/3} \tag{15}$$

where β is the slope.

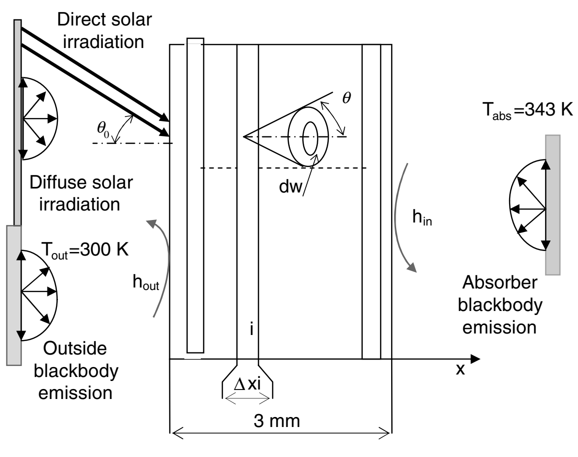

Fig. 2. Analysis model of solar collector glass cover.

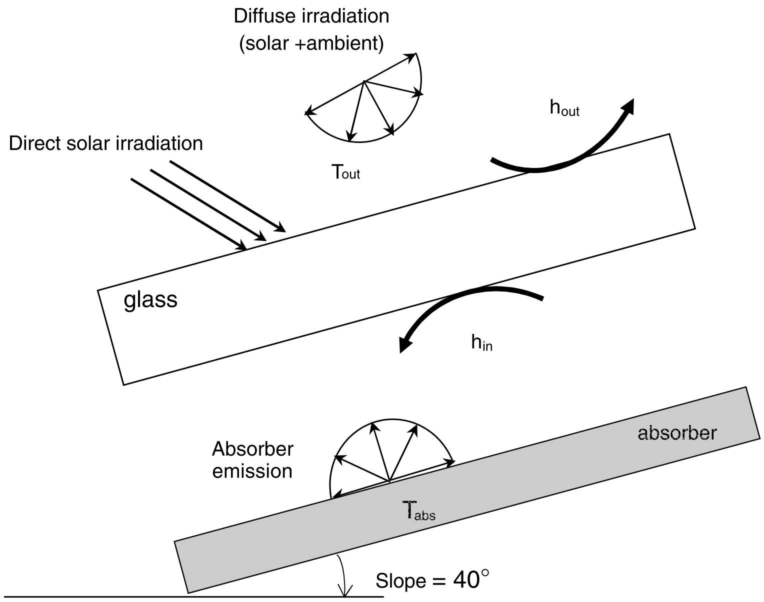

Fig. 3. Analysis model of solar collector.

The *Prandtl* number *Pr* is included in the above equation and assumed to be independent of temperature and taken equal to 0.7 (Duffie and Beckman, 1974).

The *Grashoff* number is given as

$$Gr = \frac{g|T_{\mathrm{abs}} - T_o(nl)|e_{\mathrm{air}}^3}{v^2 T_{\mathrm{air}}} \tag{16}$$

where g, v and T_{air} are the acceleration due to the gravity, kinematic viscosity of the air between the absorber and the glass cover and temperature of the air between the absorber and the glass cover, respectively. T_{abs} and $T_o(nl)$ are the absorber and the absorber side of glass temperatures, respectively.

The data used in the present study to compute the inside convective heat transfer coefficient is given by Table 1.

The one-dimensional unsteady conductive heat transfer through the glass layer is given by

$$\rho c_p \frac{\partial T}{\partial t} = \Lambda_{\mathrm{g}} \frac{\partial^2 T}{\partial x^2} + S_{\mathrm{h}} \tag{17}$$

where ρ, c, Λ_{g}, t and S_{h} are the density of the glass, specific heat of the glass, thermal conductivity of the glass, time and the heat generation source, respectively.

3. Numerical simulation

The numerical simulation has been carried out for one location at 11 a.m. on the fifth of July in Sendai city (Japan). The site characteristics and other parameters used in numerical simulation are given in Table 2. Fig. 4 shows the spectral variation of the optical constants, the real part n and the imaginary part k of the complex refractive index, for an ordinary clear glass commonly used as cover for solar collector. The curve of the real part n shows two peaks around 10 and 22 μm and the curve of the imaginary part shows two bands of strong absorption around 9.5 and 21 μm which affects the heat flux and the temperature distribution within glass layers. The non-gray model with 100 bandwidths (NG100b) contains 100 values of n and k covering the range of

Table 1
Data used to compute h_{in}

Parameter	Value	Unit
Pr	0.7	[–]
e_{air}	0.04	[m]
Λ_{air}	0.028	[W m^{-1} K^{-1}]
v	19.5×10^{-6}	[m^2 s^{-1}]
β	40	[°]

Table 2
Characteristics of the site and other parameters used in numerical simulation

Parameter	Value	Unit
Zenith angle (ζ)	19.92	[°]
Latitude	38.16	[°]
Longitude	140.51	[°]
Altitude	45.0	[m]
Day of year	186	[–]

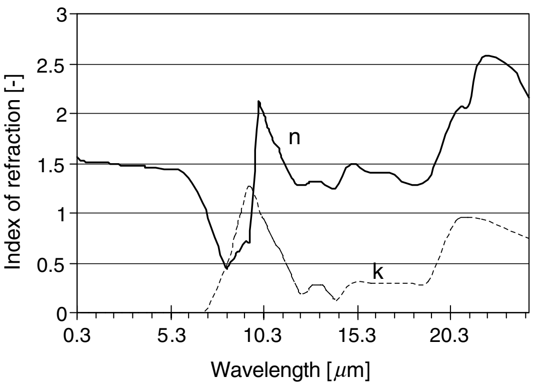

Fig. 4. Real part (n) and imaginary part (k) of the complex index of refraction of an ordinary clear glass window (NG100b model).

interest from the visible to the infrared regions (0.3–24.5 μm). These values of n and k were determined by the measurement of the reflectivity of the glass material at 45° of incidence using Fourier Transform Infrared Spectrophotometer. Fig. 5 shows the variation of n and k in term of wavelength for the non-gray model with ten bandwidths (NG10b). Fig. 6 shows the variation of n and k as a function of wavelength for a semi-gray model (SG1) that considers the glass material transparent in the visible and near infrared and almost completely opaque in the infrared region. Fig. 7 shows the variation of the optical constants of the glass as a function of wavelength for the case of another semi-gray model (SG2). SG2 model considers the glass material is almost completely transparent in the visible and near infrared and partially opaque in the infrared range. These models were applied to the solar collector glazing. The CPU times and the absolute deviations of the amount of heat fluxes of the three defined models have been compared

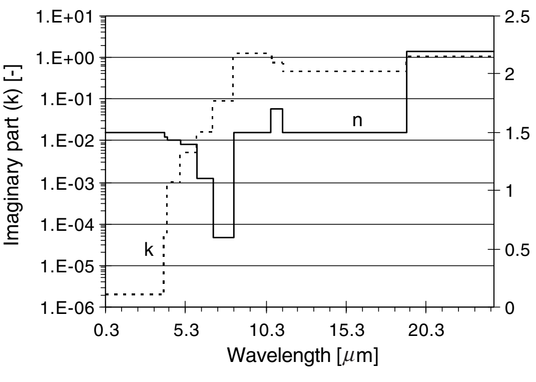

Fig. 5. Real part (n) and imaginary part (k) of the complex index of refraction of an ordinary clear glass window (NG10b model).

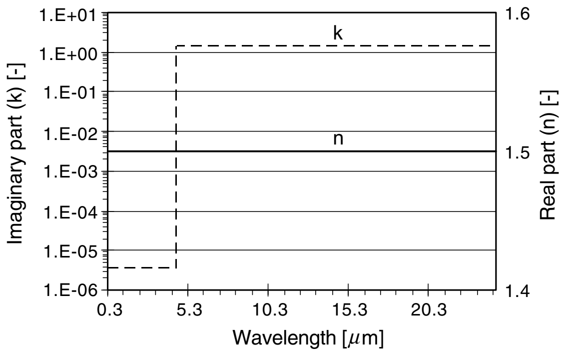

Fig. 6. Real part (n) and imaginary part (k) of the complex index of refraction of an ordinary clear glass window (SG1b model).

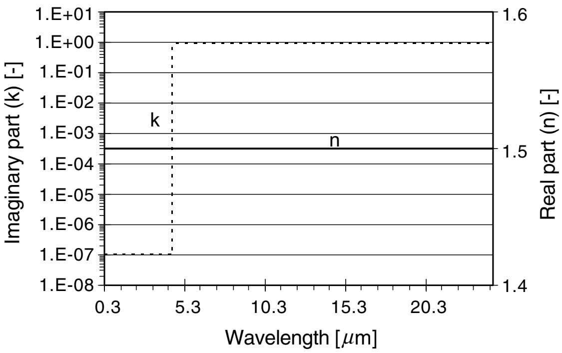

Fig. 7. Real part (n) and imaginary part (k) of the complex index of refraction of an ordinary clear glass window (SG2b model).

with the reference one (NG100b) and analysed in the following section.

4. Results and discussion

The spectral distributions of the direct solar irradiation on vertical surface, diffuse solar irradiation on horizontal surface and the incident global solar irradiation on inclined solar collector glass cover surface are shown in Fig. 8. This curve is obtained using the model of Bird and Riordan (1986) with cloudless sky conditions. The temperature distribution within the collector glass cover is plotted in Fig. 9. The gradient between the ambient and the absorber temperatures is 43 °C. Therefore, the effect of the conduction heat transfer within the glass is important compared with the radiation one. Consequently, the profiles of the temperatures distribution within a glass layer are more linear in shape. It has been shown by the authors Khoukhi et al. (2002) that, when the radiation is the dominant mode of energy

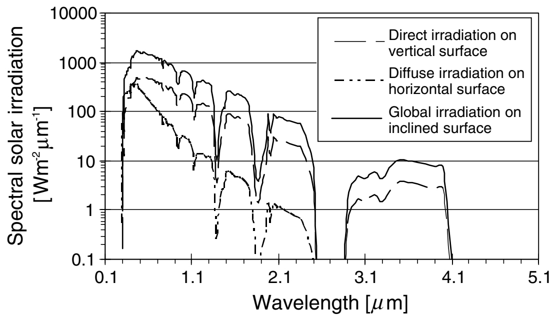

Fig. 8. Spectral distribution of the direct solar irradiation on vertical surface, diffuse solar irradiation on horizontal surface and the incident global solar irradiation on inclined surface of the solar collector glass cover.

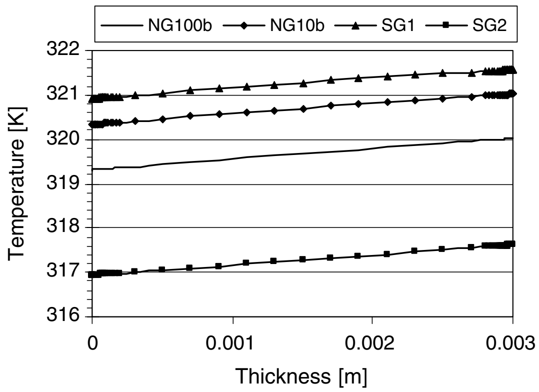

Fig. 9. Temperature distribution in the glass medium.

transfer compared with the conduction one, the profiles of the temperature within the glass layer are not linear in shape. The temperature distribution within the glass layers in case of SG1 is higher than those obtained with other models. This is due to the strong absorption, high value of k, and also to the high reflection at the internal surface of the glass which depends on the square of its real part of the complex refractive index. The radiation exiting from an interface cannot exceed that of black-body, there is an extensive energy reflection at the internal interfaces, most of it by total internal reflection (Spuckler and Siegel, 1992). Therefore, the temperature of the glass medium increases. Fig. 10 shows the heat flux within the glass medium. The amount of the heat flux within a glass layer in case of SG1 is lower than those obtained with the three other models. This is due to the strong absorption of the radiation travelling through the glass compared with SG1, NG10b and NG100b models. Therefore, one can see that for a strong absorption (case of SG1); the amount of the heat flux through the glass medium is considerably reduced. The variation of the convective heat transfer coefficients as a function of time iteration in 100 s increments is given by Fig. 11. The outside convective heat transfer coefficient is in terms of wind speed (taken for this present study equal to 1 m s^{-1}) and constant over the iteration time. For the convective heat transfer coefficient between the glass and the absorber, the shapes are the same for the four models and the steady states are reached after 1500 s for all cases. Fig. 12 shows the ratio of the CPU times and the absolute deviations of the heat fluxes amounts calculated for SG1, SG2 and NG10b from the reference model NG100b. We introduce the parameter R defined as a ratio of the CPU time consumed by the considered model to the CPU time consumed by the reference model (NG100b). In the case of semi-gray models SG1 and SG2 the CPU times are reduced to 4% of the reference computation and the absolute deviations of the heat fluxes within a glass layer compared to the reference model NG100b are 20% and 6.3%, respectively. The semi-gray model SG2 may be used for rapid preliminary calculation. In case of SG10b the CPU time is significantly reduced to less than 20% of the reference value and the absolute deviation of the steady heat flux from the reference model is only 0.3%.

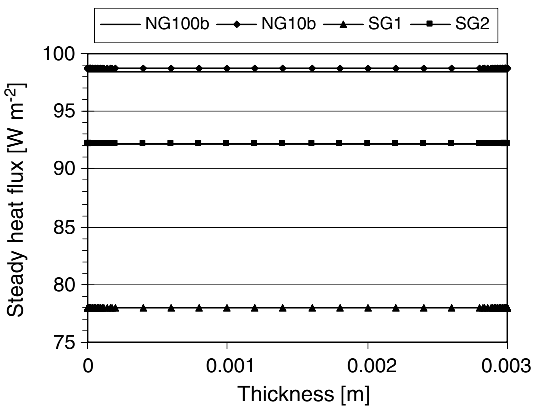

Fig. 10. Heat flux in glass medium.

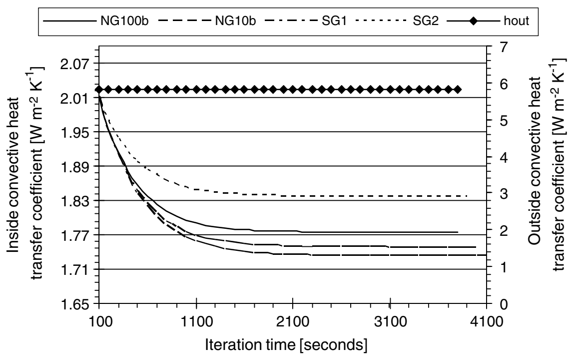

Fig. 11. Variation of the inside and outside convective heat transfer coefficients.

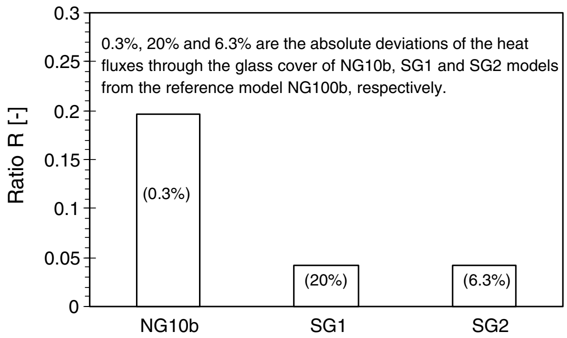

Fig. 12. *R* defined as a ratio of the CPU time consumed by the considered models to the CPU time consumed by the reference model (NG100b), and the absolute deviations of the heat fluxes of the three defined models from the NG100b.

This model could be used for simulation with the accuracy still being satisfactory.

5. Conclusions

In order to achieve more accurate modelling of a solar collector system a more rigorous radiative model must be used for the glass cover which represents the most important component of the system and greatly affects the thermal performance. Therefore, a non-gray computation procedure taking into account the absorption and emission within a glass layer is proposed.

Heat flux, temperature distribution and other heat transfer characteristics have been examined for a solar collector glass cover subjected to solar and thermal radiation. The effect of conduction and radiation on the overall heat transfer process is examined. The shape of the temperature distribution within the glass layer depends essentially on which mode of heat transfer (conduction or radiation) is the dominant one. It has been also shown that the temperature distribution in the glass layer is significantly influenced by its real and imaginary parts of the complex refractive index due to the strong absorption within a glass layer and extensive energy reflection at the internal interfaces (most of it by total internal reflection). The amount of the heat flux within a glass layer is affected by the absorption phenomenon. Indeed, for a strong absorption case the heat flux travelling though the glass is considerably reduced.

The computation has been performed for 100 values of n and k. The CPU time for the NG100b model was found to be prohibitively long. Therefore, three other models have been proposed for rapid computations (two semi-gray ones, SG1 and SG2, and one non-gray with 10 bandwidths). In the case of SG1 and SG2, the CPU times are reduced to 4% of the reference computation and the absolute deviations of the heat fluxes within a glass layer compared to the reference model NG100b are 20% and 6.3%, respectively. The semi-gray model (SG2) may be used for rapid preliminary calculations. In case of SG10b, the CPU time is significantly reduced to less than 20% of the reference value and the absolute deviation of the heat flux from the reference model is only 0.3%. Therefore, it can be concluded that the NG10b model is suitable for simulation with a very high level of accuracy. It is obvious that increasing the bandwidth number would increase the accuracy of the heat flux through the glass layer and consequently the CPU time.

The present model of the glass cover may be integrated with the absorber part of the system allowing a more rigorous simulation of the solar collector as well as solar desalination systems. In future, other models which contain more than 10 bandwidths will be investigated and with more precise values of n and k the accuracy of the model will be further improved.

References

Agarwal, V.K., Larson, D.C., 1981. Calculation of the top loss coefficient of a flat-plate collector. Solar Energy 27, 69–77.

Bird, R.E., Riordan, C., 1986. Simple solar spectral model for direct and diffuse irradiance on horizontal and tilted planes at the earth's surface for cloudless atmospheres. American Meteorological Society, 87–97.

Duffie, J.A., Beckman, W.A., 1974. Solar Energy Thermal Process. John Wiley & Sons Inc. pp. 108–119.

Howell, J.R., Bannerot, B.B., Vliet, G.C., 1982. Solar–Thermal Energy Systems. Analysis and Design. McGraw-Hill Inc. pp. 122–129.

Ho, C.-H., Ozisik, N., 1987. Combined conduction and radiation in two-layer planar medium with flux boundary condition. Numerical heat Transfer 11, 321–340.

Khoukhi, M., Maruyama, S., Sakai, S., Mori, Y., 2002. Combined non-gray conductive and radiative heat transfer simulation of a single glass window subjected to solar and thermal radiation. Solar Harvest Conference, 29th November 2002, Newcastle, Australia.

Khoukhi, M., Maruyama, S., Sakai, S., 2003. A simple method for determining the optical constants of a clear glass window using Fourier Transform Infrared Spectrophotometer. 24th Japan Symposium on Thermophysical Properties (Netsu Bussei), 6–8 October, Okayama, Japan.

Kong, H.L., Viskanta, R., 1999. Comparison of the diffusion approximation and the discrete ordinates method for the investigation of heat transfer in glass. Glastechnische. Berichte. Glass Science Technology 72 (8), 254–265.

Maruyama, S., 1997. Radiative heat transfer in a layer of anisotropic scattering fog subjected to collimated irradiation. Radiative transfer-II. Proceedings of the Second International Symposium on Radiation Transfer, pp. 157–172.

Maruyama, S., 1998. Radiative heat transfer in anisotropic scattering media with specular boundary subjected to collimated irradiation. International Journal of Heat and Mass Transfer 41, 2847–2856.

Maruyama, S., Aihara, T., 1997. Radiation heat transfer of arbitrary three-dimensional absorbing, emitting and scattering media and specular and diffuse surfaces. Journal of Heat Transfer 119, 129–136.

Spuckler, C.M., Siegel, R., 1992. Refractive index effects on radiation behaviour of heated absorbing-emitting layer. Journal of Thermophysics and Heat Transfer 6 (4), 596–604.